# Numerical investigation of interface passivation strategies for $Sb_2Se_3$/CdS solar cells

Axel Gon Medaille[1,2], Kunal J. Tiwari[1,2*], Sergio Giraldo[1,2], Marcel Placidi[2], Edgardo Saucedo[2], and Zacharie Jehl Li-Kao[2*]

1. *Institut de Recerca en Energia de Catalunya (IREC), Jardins de les Dones de Negre, 08930 Sant Adrià de Besòs, Barcelona, Spain*
2. *Electronic Engineering Department, Polytechnic University of Catalonia (UPC), c/Jordi Girona 1, 08034 Barcelona, Spain*

**Abstract:** $Sb_2Se_3$ is an emerging earth-abundant material praised for its promising optoelectronic properties, although the presence of deep interfacial defects at the vicinity of the p-n junction currently limit its performance as photovoltaic absorber. Using a device modelling approach and a realistic set of material parameters, we unravel pathways to mitigate the impact of interfacial defects with a baseline $Sb_2Se_3$/CdS device in substrate configuration. Two straightforward strategies are devised and tested against the baseline. Firstly, a thin front surface sulfurization of the $Sb_2Se_3$ absorber allowing a local lowering of the valence band and creating a "front surface field", resulting in an increased carrier selectivity and limiting the density of holes available for interface recombination, leading to a significant efficiency improvement for optimized conditions. Secondly, the use of an ultrathin insulating $Al_2O_3$ layer between the absorber and the buffer layer is considered, helping in preventing detrimental chemical interdiffusion at the junction. This strategy, already investigated in other chalcogenide-based solar cells, provides a direct interface passivation, though the interlayer thickness needs a fine tuning to balance the benefits of reduced interface recombination and a detrimental $Al_2O_3$ low-conductivity layer. In each case, an analysis covering a broad range of parameters is presented, and conclusions are made in the frame of past numerical and experimental results.

*Keywords:* *$Sb_2Se_3$, SCAPS-1D, device simulation, defects, passivation*

**Introduction:**

Low-cost, low-toxicity and high-efficiency materials are key to the success and future large-scale deployment of thin film solar cells. $Sb_2Se_3$ seems to fit those criteria being an earth-abundant material with an optical bandgap between 1.1-1.3 eV, high absorption coefficient (>$10^5$ $cm^{-1}$), high carrier mobility (15 and 40 cm/Vs for electrons and holes respectively)[1,2]. With covalently bonded $(Sb_4Se_6)_n$ ribbons growing along the c-axis and linked by van der Waals force along the a-axis and b-axis, this quasi-1D material offers potentially remarkable anisotropic carrier transport properties[3]. While those ribbons are bonded by Van der Walls interaction, Sb and Se are covalently bonded enabling a very effective carrier transport along the c-axis. Unlike $CuInGaSe_2$ (CIGS) and $Cu_2ZnSn(S,Se)_4$ (CZTSSe), antimony selenide

Kunal.tiwari@upc.edu
Zacharie.jehl@upc.edu

($Sb_2Se_3$) is a binary compound allowing several synthesis methods to be developed: closed-space sublimation (CSS), vapor transport deposition (VTD), co-evaporation, sputtering, electrochemical deposition[1,2,4–6]. Additionally, $Sb_2Se_3$ solar cells benefit from optimizations strategies previously used in other more mature chalcogenide technologies, such as the widespread use of CdS as n-partner layer. However, experimental studies report a large $V_{OC}$ deficit and limited efficiency in comparison with its Shockley-Queisser limit (33%) and other more mature chalcogenide materials. In that regard, this limitation is commonly ascribed to the presence of bulk and interfacial defects[1,5,7–9]. In a recent study[10], the individual influence of the three most commonly reported defects (D1 and D2, bulk; D3, interfacial) investigated by numerical analysis was reported. The complete set of parameters reported on these defects can be found in the supplementary information Table S 2. A comprehensive overview on the origin of defects existing in $Sb_2Se_3$ based solar cells can be in found in reference[11], while reference[12] specifically reports on the existence of a deep defect at 0.39eV, with a concentration possibly as high as $10^{17}.cm^{-3}$. It was additionally demonstrated[10] that interfacial defects D3, specific to the $Sb_2Se_3$/CdS interface, were markedly prevalent and severely limiting the voltage and fill factor of the device, and to a lesser extent, the short circuit current. Using a thin interfacial $SnO_2$ layer after the CdS proved beneficial to both experimental and simulated devices in passivating the pn interface.

In this work, we propose to use numerical modelling to assess two alternative strategies, each with its own merits, to efficiently passivate the pn interface. SCAPS-1D[13] software is used to simulate the performance of Mo/$MoSe_2$/ $Sb_2(S,Se)_3$/CdS/ZnO/ZnO:Al solar cells in substrate configuration with most of the baseline solar cell parameters used in our model being from in-lab characterizations, though the defect parameters of D1, D2 and D3 are taken similar to reference[10] to ensure an accurate comparability between both studies. In a first step, we investigate how the surface sulfurization of a bare $Sb_2Se_3$ absorber can electrically passivate the $Sb_2(S,Se)_3$/CdS interface, through the creation of a “front surface field”. The substitution of Se by S atoms locally increases the bandgap and lowers the valence band. This results in an enhanced repelling of the holes from the pn junction, and thus increasing the carrier selectivity and preventing carrier recombination to occur at the interface. Strategies using sulfur as a grading element are just starting to be investigated for improving $Sb_2Se_3$-based solar cells, notably using a so-called “V-shape grading” [14], as well as to improve the pn interface [15]. However, the exact mechanism through which a front sulfur grading improves the interface remains unexplained. We demonstrate here that the lowering of the valence band suffices to efficiently repel holes from the pn interface, similar to the well-known back surface field effect for electrons. While possible beneficial or detrimental effects of S from a material and interface defect viewpoint may exist, it is not necessary to explain how front sulfurization improves the performance of photovoltaic devices. Additionally, it is shown that a steep grading of less than 100 nm appears to yield the strongest passivating effect on interface defects, without the drawbacks which arise for higher sulfur content. In a second part of this work, the use of a direct amorphous $Al_2O_3$ passivating oxide layer blocking elemental interdiffusion is considered. In this configuration, the interface defect density is considered reduced[16,17], but the introduction of an intrinsic wide bandgap layer can conversely prove detrimental to carrier transport across the junction. By varying the interfacial $Al_2O_3$ thickness, it is demonstrated that while a decrease in the FF can be linked to the introduction of an $Al_2O_3$ interlayer, the beneficial effect of passivating the interface markedly improves the performance, and thicknesses in the 5 nm range appear as an experimentally feasible compromise. This study is a complement to previous investigations related to the limitations of this class of solar cells, and provides insights in both straightforward and realistic pathways to enhance the conversion efficiency of state-of-the-art $Sb_2Se_3$-based photodiodes using CdS as buffer layer.

Kunal.tiwari@upc.edu
Zacharie.jehl@upc.edu

**Materials and Methods:**

SCAPS 3.08 is used to perform the numerical modelling in this study[13]. The solar cell structure is built as follows: Mo/$MoSe_2$/$Sb_2(S,Se)_3$/CdS/ZnO/ZnO:Al. The baseline parameters, including the D1, D2 and D3 defects, are summarized in the supplementary information of this work Table S 1 and Table S 2, and are a combination of literature data[10] and in-lab characterizations[6,18]. The introduction of a back $MoSe_2$ layer acts as an electron blocking layer, thus suppressing the influence of the back contact on the presented results as we focus on the pn interface. This model does not aim at being fully quantitative, and the optical properties (front transmission, back reflectivity) are not calculated here; similarly, the layer specific absorption is calculated following a square root law of the bandgap rather than from an experimental optical index. The modelling of the surface sulfurization is achieved by duplicating the absorber layer and introducing a parabolic composition grading, as often experimentally reported[19], ranging from pure selenium $Sb_2Se_3$ to pure sulfur $Sb_2S_3$. The two parameters being simultaneously adjusted are the thickness of the sulfurized layer, varied from 0 to 750 nm, and the front sulfur content, varied from 0 (pure Se) to 1 (pure S), which corresponds approximatively to a downshift of the valence band by 300 meV.

In the second part of the study, an ultrathin amorphous $Al_2O_3$ interfacial layer is introduced between the absorber and the CdS buffer layer, which is considered here as perfectly effective for quenching the D3 defect specific to the $Sb_2Se_3$/CdS interface. The thickness of the $Al_2O_3$ interfacial layer is varied from 0 nm to 10 nm to assess a possible degradation of the PV performance, and the corresponding photovoltaic figures of merits are modelled along with the quantum efficiency.

**Results and Discussion:**

Using a combination of in-lab measured data and literature, a baseline pure Se $Sb_2Se_3$ solar cell is established as previously described and used throughout the present study. To assess the reliability of our model, a comparative investigation similar to that of reference[10] is made and described in the supplementary information Table S 3, with the individual influence of D1, D2 and D3 being evaluated. The results appear very consistent with those from reference[10], with interface defects being the main factor limiting the conversion efficiency of the cells, thus validating the consistency of our baseline model with previous reports.

Defective interface such as the one simulated by the defect D3 can be passivated by various means, among which two are presented here. Firstly, we focus on demonstrating that creating a “front surface field” in the valence band, at the vicinity of the pn interface, is a very efficient way to repel holes from the junction and thus significantly reduce interface recombination. This approach can be viewed as an electric field passivation. A similar process is routinely and successfully used in the highest performing CIGSe solar cells[20,21]. Hence, we modelled the effect of a sulfur passivated $Sb_2(S,Se)_3$ graded in composition toward pure $Sb_2S_3$. It should be noted that $Sb_2S_3$ presents a similar Q1D crystallographic structure as $Sb_2Se_3$. The introduction of additional defects due to lattice mismatch is therefore expected to be minimal, especially in such ultrathin configuration, and will be thus be ignored in the model. This surface sulfurization lowers the energy position of the valence band to repel holes from the pn interface.

The baseline PV parameters (no surface sulfurization) are $V_{oc}$ = 480 mV, FF = 66.3%, $J_{sc}$ = 35.4 mA.cm$^{-2}$ and Eff = 11.3%. By varying simultaneously the sulfurization depth (x-axis, Figure 1) and the front sulfur content

Kunal.tiwari@upc.edu
Zacharie.jehl@upc.edu

(y-axis, Figure 1), we obtain surface plots of the $V_{oc}$, FF, $J_{sc}$ and Efficiency. As expected, increasing the S content reduces the current while increasing the voltage. Importantly, we note that varying the thickness for a fixed surface composition only marginally changes the voltage, except for extreme values where the absorber becomes close to pure S. This indicates that the benefits of sulfurization are mostly related to passivating the pn interface and the increase in voltage is achieved even for an ultrathin sulfurized layer. Comparatively, the variations in $J_{sc}$ appear to be driven by both the thickness of the sulfurized layer and the surface composition. This can easily be understood in term of spectral absorption as that a thicker sulfurized layer reduces the total narrow bandgap region extent and thus limits the absorption of low energy photons. Similarly to the voltage, the Fill Factor is also less affected by the thickness of the sulfurized layer than by the front S content, which is consistent with a system limited by interface recombination. An optimum FF = 77% value is obtained for a surface sulfur composition in the 0.3-0.7 range. Hence, while the FF follows the $V_{oc}$ in a sense that both figures of merit are limited by interface recombination, it is simultaneously driven by the interface band matching between $Sb_2(S,Se)_3$ and CdS. The calculated conversion efficiency appears mostly independent from the thickness of the sulfurized layer, while strongly depending on the sulfur content at the interface with optimum efficiencies above 17% obtained in the range of 50%-70% front sulfur content and for a sulfurization depth lower than 200 nm. In conclusion, it appears that the experimentalist ought to optimize the front sulfur content at a relatively high level (around 60%) rather than the overall sulfurized layer thickness to tackle the issue of interfacial defects, and working with thin or ultrathin sulfurized layer may be preferable from an experimental viewpoint to avoid disrupting too much the fabrication process, along with yielding higher performance from a simulation viewpoint. Indeed, sulfurization thicknesses significantly larger than the space charge region extent will conversely slightly affect the electronic transport in the conduction band. In this model, optimum conditions are found for a front sulfur content in the 60 to 80% range, and a sulfurized thickness in the 50 nm to 100 nm range. Post deposition surface sulfurization methods such as reported in the CIGSe field[19] should be the favored, as those have proven their reliability to obtain such tunable and steeply graded profile.

Kunal.tiwari@upc.edu
Zacharie.jehl@upc.edu

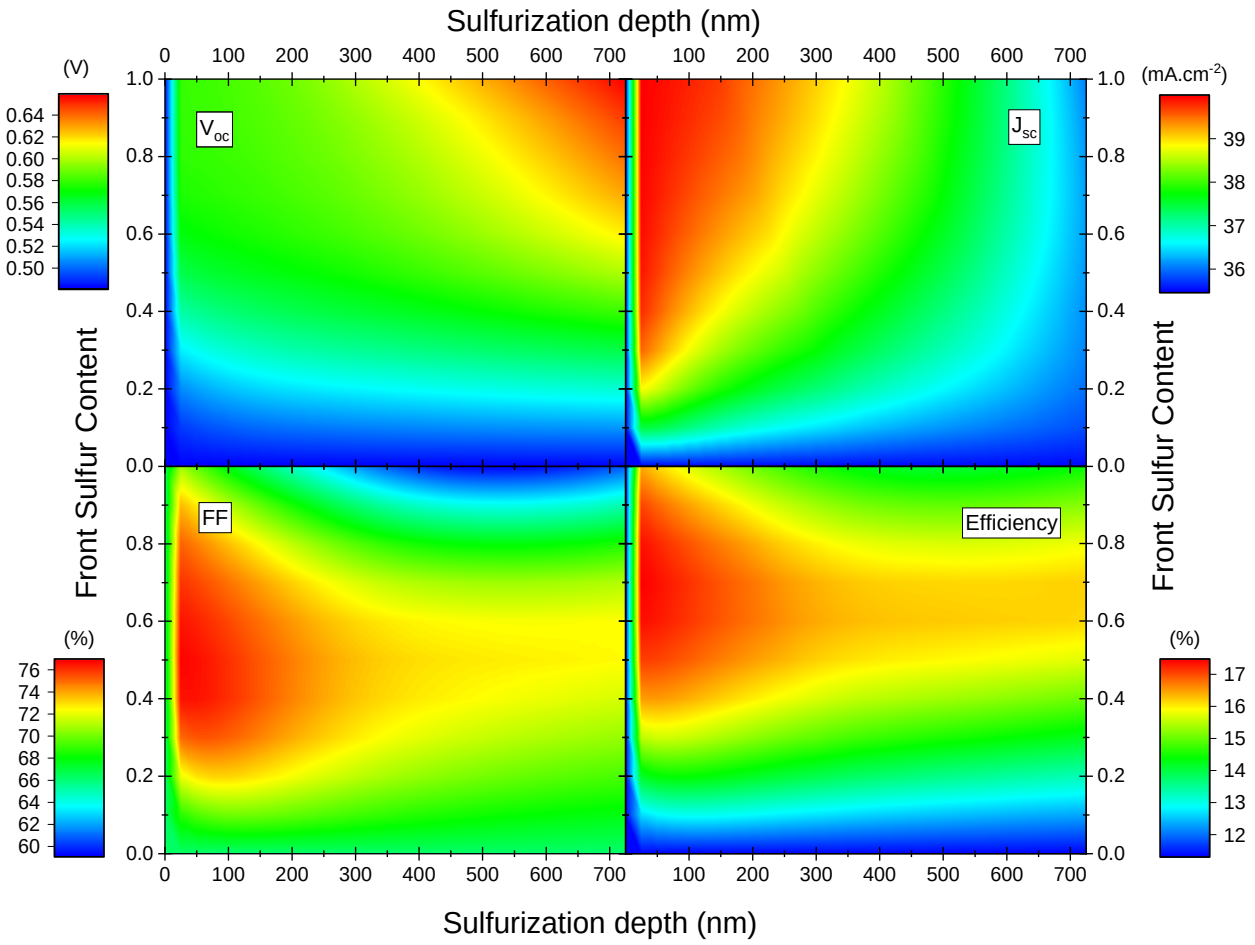


*Figure 1 Modelled figures of merits of $Sb_2(S,Se)_3$ solar cells with varying the front sulfur content (y-axis) and the sulfurization depth (x-axis).*

Using a front S content of 0.7 and a sulfurization depth of 80 nm, in Figure 2 we compare the quantum efficiency with that of the non-sulfurized baseline $Sb_2Se_3$ solar cell. In the case of the baseline, the quantum efficiency reaches a value around 80% in the visible range (with the exception of the 400-500 nm due to CdS absorption); the EQE curve even increases with the wavelength, which is a clear indication of a device limited by front interface recombination. It should be noted that in a real device however, such feature would hardly be observed as back interface recombination (quenched in the model) would counterbalance the long wavelength EQE increase. The sulfur-graded $Sb_2(S,Se)_3$ solar cell shows a quantum efficiency starting close to 100% (reflection losses are ignored in this model) in the 500 – 800 nm range before progressively converging with the baseline QE in the infrared region at 1100 nm. The EQE difference showed on the same Figure 2 (right y-axis) offers a clearer view on how reducing interface recombination primarily affects photocarriers from high energy photons, consistently with the reported effect of passivating interface defects[22]. As D3 interacts in a comparable manner with electrons and holes, being located close to the middle of the bandgap, it also acts as a recombination center and not just a carrier trap affecting the voltage. By drifting holes from the pn junction, the front interface recombination rate is almost completely quenched as illustrated in Figure 3a comparing the interface recombination

Kunal.tiwari@upc.edu
Zacharie.jehl@upc.edu

currents. The reduction in hole density at the vicinity of the pn interface is also clearly visible when plotting the spatial distribution of hole density in the supplementary information, Figure S 1. The decrease of the interface recombination current with the voltage from 4.5 mA.cm$^{-2}$ for 0V perfectly matches the short circuit current difference $\Delta J_{sc}$ between both conditions as shown in Figure 3. Additionally, the difference in interface recombination currents increases up to 12 mA.cm$^{-2}$ for 0.41 V (maximum power point for the baseline conditions) which can directly be correlated with the observed loss of FF without surface sulfurization (66% vs 76% for the optimized sulfurized case respectively). Therefore, surface sulfurization not only favors a higher short circuit current and voltage, but also completely eliminates the FF losses linked to interface recombination.

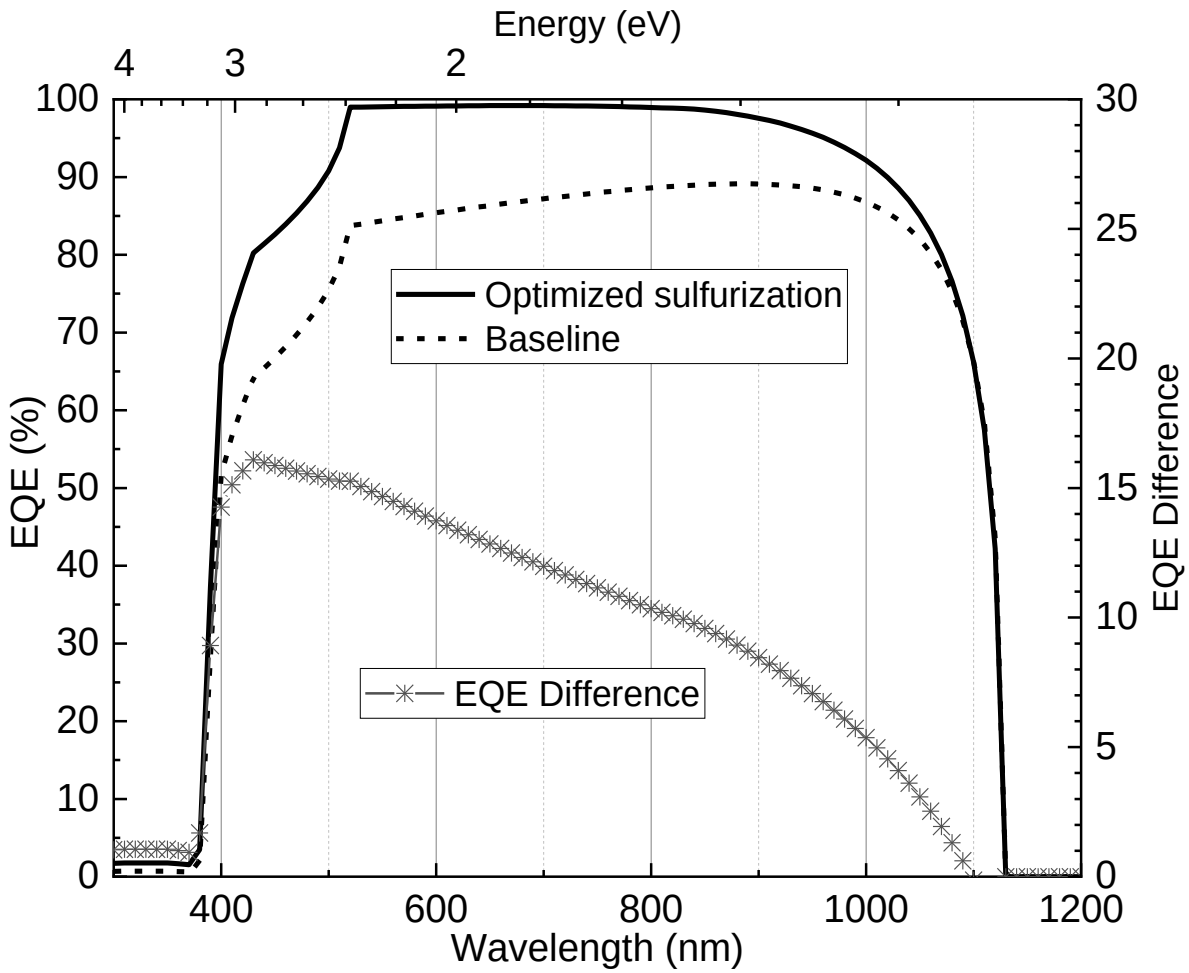


*Figure 2 Modelled EQE (left y-axis) for baseline conditions (dashed line) and optimized sulfurization conditions (80 nm, 0.7 S content, solid line). The difference between both curves is plotted on the right hand y-axis (star symbol).*

Kunal.tiwari@upc.edu
Zacharie.jehl@upc.edu

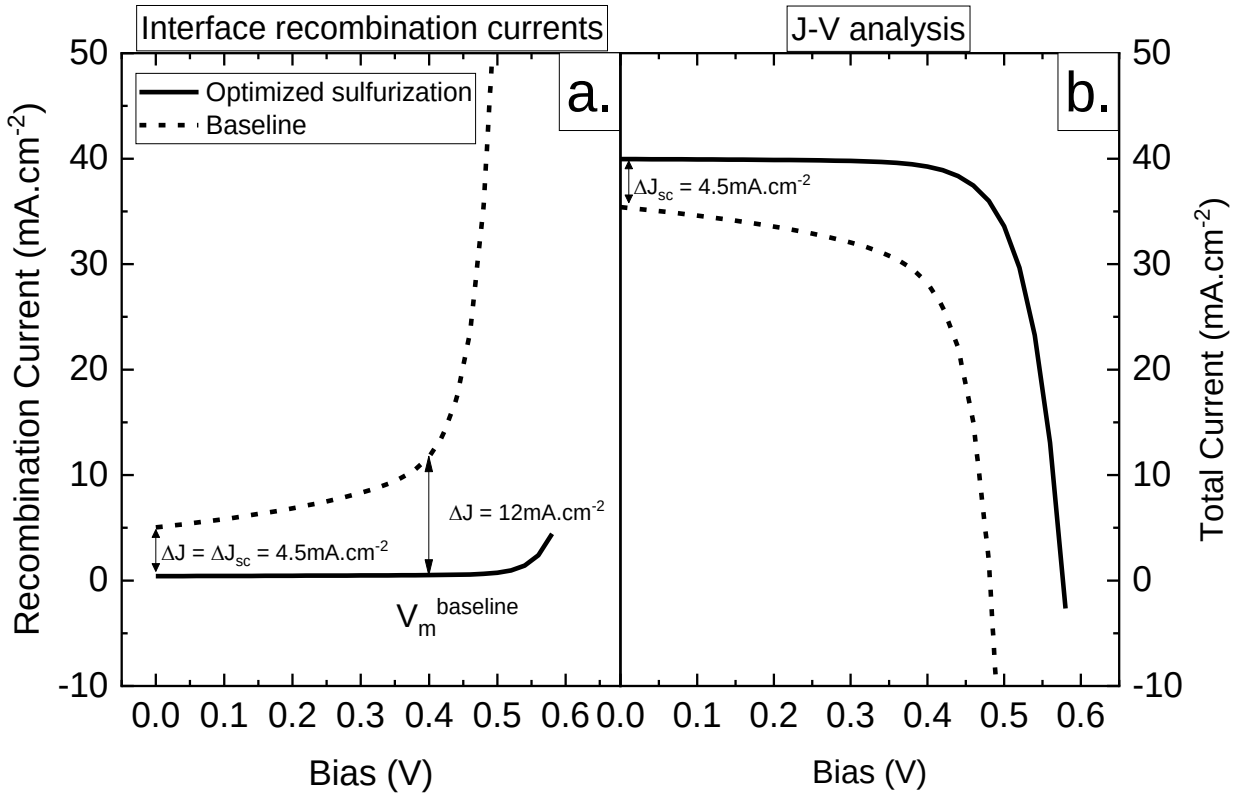


*Figure 3 a: modelled interface recombination currents for baseline conditions (dashed line) and optimized sulfurization conditions (solid line); b: corresponding J-V curves.*

While surface sulfurization appears, under properly optimized conditions, as an efficient way to reduce or possibly suppress the influence of the interfacial D3 defect on the PV performance, its experimental implementation may prove challenging as it requires sulfurizing an already formed $Sb_2Se_3$ absorber and it remains to be seen whether a similar level of tailoring (steep surface grading) can be achieved in Q1D materials. A more straightforward and already experimentally investigated [16,17] approach consists in using a passivation layer in the form of a well-controlled, ultrathin large bandgap oxide such as $Al_2O_3$. Admitting that such interlayer can indeed perfectly passivate the interface defects by preventing elemental interdiffusion between the $Sb_2Se_3$ absorber and the CdS buffer layer, the question remains whether the electron transport across the pn junction would be negatively impacted by the presence of a low conductivity interlayer.

Solar cell simulations were done while modifying the thickness of $Al_2O_3$ layer from 0 to 10 nm as shown in Figure 4, considering an ideal passivation of the interface defects D3. Expectedly, the latter leads to a sharp performance improvement with the efficiency reaching a value close to 17% for an ultrathin (but experimentally challenging) 1 nm $Al_2O_3$ layer; specifically, the PV figures of merit closely resemble those of the optimized front sulfurization conditions, confirming that both approaches can be equivalent in terms of surface defect passivation. As $Al_2O_3$ does not introduce additional recombination mechanism nor detrimental Fermi level pinning, the voltage and current remain unaffected by variations of the $Al_2O_3$ thickness up to 10 nm. However, the introduction of a high electron barrier of low conductivity impacts the Fill Factor through series resistance, with a value decreasing from 74 % (1 nm $Al_2O_3$) down to 66% (10

Kunal.tiwari@upc.edu
Zacharie.jehl@upc.edu

nm $Al_2O_3$), leading to a degradation of the efficiency down to 15.2%, a value remaining nevertheless much higher than the 11.3% baseline without $Al_2O_3$. It thus appears that, from an experimental viewpoint, there exists a small margin in the fabrication of the $Al_2O_3$ interlayer before markedly degrading the performance, though obtaining a perfect coverage and homogeneity with 1 nm may be challenging and larger thicknesses will possibly have to be targeted. The modelled quantum efficiency including a thin 5 nm $Al_2O_3$ interlayer is presented in the supplementary information Figure S 2 and compared to the baseline EQE, along with the EQE difference which allows to clearly visualize that once again, most of the improvement from passivating the interface defect D3 occurs in the high energy part of the spectrum. While both approaches have their merits and possibly lead to a similar outcome, significantly improving the PV performance of a baseline $Sb_2Se_3$ solar cell by alleviating the limitations stemming from the D3 interface defect, it appears that surface sulfurization has the edge in terms of performance while being possibly easier to achieve experimentally, as a comfortable margin exists in the tailoring of the surface sulfur composition grading. The present study however, still overlooks a few key aspects detailed below for which additional experimental data will be required.

**Limitations and future improvements:**

The main limitation of this work is the assumption made that neither sulfurization nor $Al_2O_3$ introduce new defects at the pn interface. Experimentally, our current work focuses on the deposition of amorphous $Al_2O_3$ layers by either evaporation[17] or Atomic Layer Deposition, albeit on Kesterite absorbers for now, and no additional defects were detected so far. To not degrade the crystalline quality of the $Sb_2Se_3$ absorber, it is recommended to focus primarily on low temperature deposition of amorphous $Al_2O_3$. In this simulation discussed here, D3 is considered fully passivated as long as $Al_2O_3$ is intercalated between the absorber and the CdS, and while the use of intrinsic oxide layers has often proven effective in improving defective interfaces in chalcogenide solar cells, a thorough characterization work on such interface would be necessary to get a more accurate representation of real devices. The information given by the current study merely states that in the thickness range considered, the additional series resistance from the $Al_2O_3$ layer would have a limited yet measurable impact on the performance for layers below 5 nm.

This work proves that the beneficial effect of sulfurization can be solely explained by the valence band grading at the pn interface. However, this model is not designed to discuss the possible (and likely) chemical interaction of S with the $Sb_2Se_3$ film, which may result in further beneficial or detrimental modifications of the interface. The possibility of additional defects being introduced by sulfurization cannot be discarded at this point, though no consensus currently exists in that regard. Once again, the model would strongly benefit from additional experimental data, specifically regarding the $Sb_2Se_3$/$Sb_2S_3$/CdS stack. Our group currently investigates the defect profile of experimental $Sb_2(S,Se)_3$ solar cells using various methods, among which Photothermal Deflection Spectroscopy (PDS). While interesting results have indeed been obtained, and could have been used in this work, those remain at a stage too preliminary and relatively incomplete. It was thus decided to instead make use of the currently more reliable data reported in reference[10], which also ensures that the results from both works remain easily comparable.

Finally, this work assumes that CdS is used as buffer, owing to its proven efficacy and reliability on chalcogenide solar cells. However, the D3 defects has so far been only reported for this specific interface,

Kunal.tiwari@upc.edu
Zacharie.jehl@upc.edu

and it is obvious that alternative buffer layers will be (and already are) investigated. Nevertheless, the ideas developed in this work would remain valuable even in a different context. Surface sulfurization especially may be buffer-agnostic, providing an electric-field interface defect passivation from within the absorber layer.

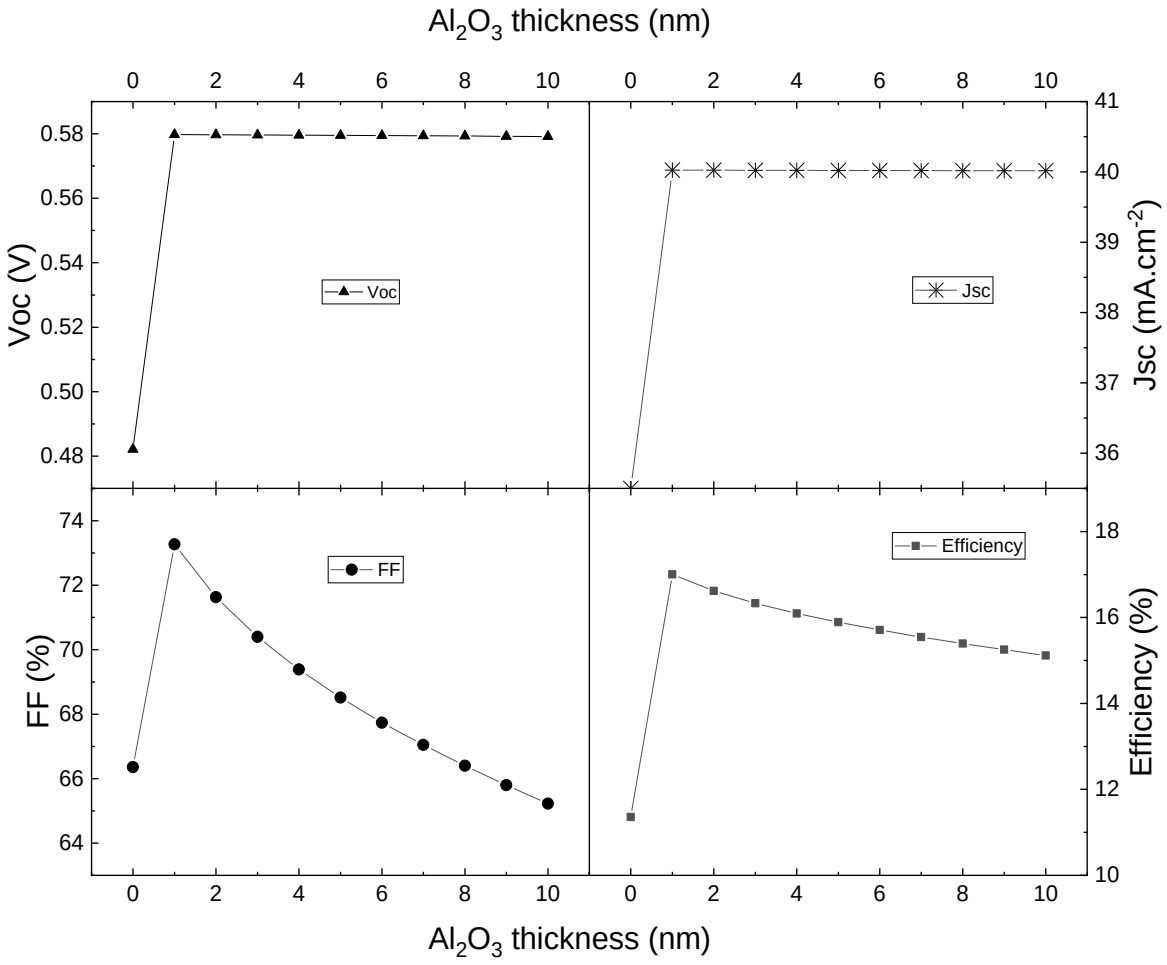


*Figure 4 Evolution of the calculated PV parameters when increasing the $Al_2O_3$ interlayer thickness.*

**Conclusion:**

Using a numerical modelling approach, we first established a baseline for a state-of-the-art $Sb_2Se_3$ solar cell fabricated in the substrate configuration, and investigated its main limitations through the three most commonly reported defects. The results obtained are in perfect agreement with the previous reports, as interface defects appear to be the main limiting factor for this type of solar cells. We thus propose two simple strategies to tackle this issue and markedly improve the photovoltaic performance. Firstly, we demonstrate how a surface sulfur gradient can create a "front surface field" for the holes, thus reducing interface recombination, and that such effect is sufficient to completely quench interface recombination. We show that while the surface sulfur content is a major performance driver, with an efficiency rising up to 17% (from 11.3% for the baseline), the thickness of the sulfurized layer is on the other hand of slightly

Kunal.tiwari@upc.edu
Zacharie.jehl@upc.edu

lesser importance. Therefore, we devise that from an experimental viewpoint, working with thin, steeply S-graded sulfurized layers is preferable. In a second part of this work, an ultrathin, low conductivity $Al_2O_3$ interlayer is introduced at the absorber/CdS interface. While the possible beneficial effect of limited elemental interdiffusion cannot be taken into account here, we still observe a radical performance improvement as compared to the baseline device up to 17-15% if assuming that D3 is quenched, though increasing the interlayer thickness from 1 nm up to 10 nm will affect the performances. We thus believe that for an experimentalist opting for this passivation strategy, there is a relatively comfortable thickness margin for performance optimization.

In conclusion, both approaches yield a somewhat similar trend and appear valid to tackle the issue of interface recombination. Much work remains to be done for the emerging $Sb_2Se_3$ solar cells to overcome their current limitations and approach the PV performance of the more mature chalcogenide counterparts. Nevertheless, this work argues that approaching the 17% efficiency threshold is experimentally possible in the near future through the implementation of simple strategies, which have often proven their worth in other technologies.

## *Acknowledgements*

The authors wish to thank Prof. Marc Burgelman, for his invaluable contribution to the field of photovoltaics by designing the program SCAPS, now widely used by various research groups around the world.

The authors acknowledge the European Research Council ERC-CoG grant SENSATE (Grant agreement ID: 866018) for the financial support of this work.

This work is part of the R+D+i MaterOne project Ref. PID 2020-116719RB-C41 funded by MCIN/AEI/10.13039/5011000110033.

Professor Marcel Placidi acknowledges the Spanish Ministry of Science and Innovation (MCIN) for the financial support in the frame of the Ramon y Cajal program (RYC-2017-23758).

## *References*

1. Tang, R. *et al.* Highly efficient and stable planar heterojunction solar cell based on sputtered and post-selenized Sb2Se3 thin film. *Nano Energy* **64**, 103929 (2019).
2. Mavlonov, A. *et al.* A review of Sb2Se3 photovoltaic absorber materials and thin-film solar cells. *Solar Energy* **201**, 227–246 (2020).
3. Zhou, Y. *et al.* Thin-film Sb2Se3 photovoltaics with oriented one-dimensional ribbons and benign grain boundaries. *Nature Photon* **9**, 409–415 (2015).

Kunal.tiwari@upc.edu
Zacharie.jehl@upc.edu

4. Zhang, J. *et al.* Alternative back contacts for Sb2Se3 solar cells. *Solar Energy* **182**, 96–101 (2019).
5. Liang, G.-X. *et al.* Sputtered and selenized Sb2Se3 thin-film solar cells with open-circuit voltage exceeding 500 mV. *Nano Energy* **73**, 104806 (2020).
6. Vidal-Fuentes, P. *et al.* Efficient Se-Rich Sb2Se3/CdS Planar Heterojunction Solar Cells by Sequential Processing: Control and Influence of Se Content. *Solar RRL* **4**, 2000141 (2020).
7. Chen, C. & Tang, J. Open-Circuit Voltage Loss of Antimony Chalcogenide Solar Cells: Status, Origin, and Possible Solutions. *ACS Energy Lett.* **5**, 2294–2304 (2020).
8. Williams, R. E. *et al.* Evidence for Self-healing Benign Grain Boundaries and a Highly Defective Sb2Se3–CdS Interfacial Layer in Sb2Se3 Thin-Film Photovoltaics. *ACS Appl. Mater. Interfaces* **12**, 21730–21738 (2020).
9. Dong, J., Liu, Y., Wang, Z. & Zhang, Y. Boosting $V_{OC}$ of antimony chalcogenide solar cells: A review on interfaces and defects. *Nano Select* nano.202000288 (2021) doi:10.1002/nano.202000288.
10. Chen, Y. *et al.* Importance of Interfacial Passivation in the High Efficiency of $Sb_2Se_3$ Thin-Film Solar Cells: Numerical Evidence. *ACS Appl. Energy Mater.* **3**, 10415–10422 (2020).
11. Spalatu, N. *et al.* Screening and optimization of processing temperature for Sb2Se3 thin film growth protocol: Interrelation between grain structure, interface intermixing and solar cell performance. *Solar Energy Materials and Solar Cells* **225**, 111045 (2021).
12. Krautmann, R. *et al.* Analysis of grain orientation and defects in Sb2Se3 solar cells fabricated by close-spaced sublimation. *Solar Energy* **225**, 494–500 (2021).
13. Burgelman, M., Nollet, P. & Degrave, S. Modelling polycrystalline semiconductor solar cells. *Thin Solid Films* **361–362**, 527–532 (2000).
14. Li, K. *et al.* Over 7% Efficiency of Sb2 (S, Se) 3 Solar Cells via V-Shaped Bandgap Engineering. *Solar RRL* **4**, 2000220 (2020).

Kunal.tiwari@upc.edu
Zacharie.jehl@upc.edu

15. Chen, S. *et al.* Improved Open-Circuit Voltage of Sb2Se3 Thin-Film Solar Cells Via Interfacial Sulfur Diffusion-Induced Gradient Bandgap Engineering. *Solar Rrl* **5**, 2100419 (2021).

16. Phillips, L. J. *et al.* Current Enhancement via a TiO2 Window Layer for CSS Sb2Se3 Solar Cells: Performance Limits and High Voc. *IEEE Journal of Photovoltaics* **9**, 544–551 (2019).

17. Ojeda-Durán, E. *et al.* CZTS solar cells and the possibility of increasing VOC using evaporated Al2O3 at the CZTS/CdS interface. *Solar Energy* **198**, 696–703 (2020).

18. Tiwari, K. J. *et al.* Efficient Sb2Se3/CdS planar heterojunction solar cells in substrate configuration with (hk0) oriented Sb2Se3 thin films. *Solar Energy Materials and Solar Cells* **215**, 110603 (2020).

19. Kobayashi, T. *et al.* Impacts of surface sulfurization on Cu(In1−x,Gax)Se2 thin-film solar cells. *Progress in Photovoltaics: Research and Applications* **23**, 1367–1374 (2015).

20. Nakada, T. *et al.* Improved Cu(In,Ga)(S,Se)2 thin film solar cells by surface sulfurization. *Solar Energy Materials and Solar Cells* **49**, 285–290 (1997).

21. Nakamura, M. *et al.* Cd-Free Cu(In,Ga)(Se,S)2 Thin-Film Solar Cell With Record Efficiency of 23.35%. *IEEE Journal of Photovoltaics* **9**, 1863–1867 (2019).

22. Mackel, H. & Cuevas, A. Determination of the surface recombination velocity of unpassivated silicon from spectral photoconductance measurements. in *Proceedings of 3rd World Conference onPhotovoltaic Energy Conversion, 2003* vol. 1 71-74 Vol.1 (2003).

Kunal.tiwari@upc.edu
Zacharie.jehl@upc.edu

# Supplementary information

1. Modelling parameters

## 1.1 Materials

| | $Sb_2Se_3$ | $Sb_2S_3$ | CdS | i-ZnO | ZnO:Al |
|---|---|---|---|---|---|
| Thickness (nm) | 0-750 | 0-750 | 60 | 100 | 300 |
| Eg (eV) | 1.1 | 1.7 | 2.4 | 3.3 | 3.3 |
| $\chi$(eV) | 4.04 | 3.7 | 4.2 | 4.45 | 4.45 |
| $\varepsilon_r$ (eV) | 18 | 7 | 10 | 9 | 9 |
| $\mu_e$ ($cm^2.V^{-1}.s^{-1}$) | 15 | 50 | 100 | 100 | 100 |
| $\mu_h$ ($cm^2.V^{-1}.s^{-1}$) | 5 | 5 | 10 | 25 | 25 |
| $N_a$ ($.cm^{-3}$) | 1.00E+13 | 1.00E+13 | - | - | - |
| $N_d$ ($.cm^{-3}$) | - | - | 5.00E+17 | 1.00E+18 | 1.00E+20 |

*Table S 1 Modelling material parameters*

## 1.2 Defects

| | D1 | D2 | D3 |
|---|---|---|---|
| Position | bulk | bulk | pn interface |
| type | Neutral | Neutral | Neutral |
| $\sigma_e(cm^2)$ | 1.20E-14 | 2.60E-15 | 2.30E-17 |
| $\sigma_h(cm^2)$ | 1.20E-14 | 2.60E-15 | 2.30E-17 |
| Distribution | Gauss | Gauss | Gauss |
| Energy above VB (eV) | 0.363 | 0.398 | 0.43 |
| Char. energy (eV) | 0.1 | 0.1 | 0.1 |
| Total density ($.cm^{-3}$) | 2.50E+14 | 6.40E+14 | 7.30E+15 |
| Peak density ($.cm^{-3}$) | 1.41E+15 | 3.60E+15 | 4.12E+16 |

*Table S 2 Modelling absorber defect parameters.*

Kunal.tiwari@upc.edu
Zacharie.jehl@upc.edu

2. Baseline defects: influence on PV parameters

| Configurations | $V_{oc}$ (V) | $J_{SC}$ (mA/cm$^2$) | FF (%) | PCE (%) |
|---|---|---|---|---|
| w/o D1, D2, D3 | 0.73 | 40.5 | 85 | 25.4 |
| w/ D1 only | 0.6 | 40.5 | 76.8 | 18.6 |
| w/ D2 only | 0.62 | 40.5 | 77 | 19.3 |
| **w/ D3 only** | **0.48** | **35.4** | **66.9** | **11.5** |
| w/ D1 & D2 | 0.58 | 40.5 | 76 | 17.8 |
| **w/ D1, D2, D3** | **0.48** | **35.4** | **66.3** | **11.3** |

*Table S 3 Influence of baseline defects on Sb2Se2 solar cells' photovoltaic parameters.*

3. Hole density at the pn interface with and without sulfurization

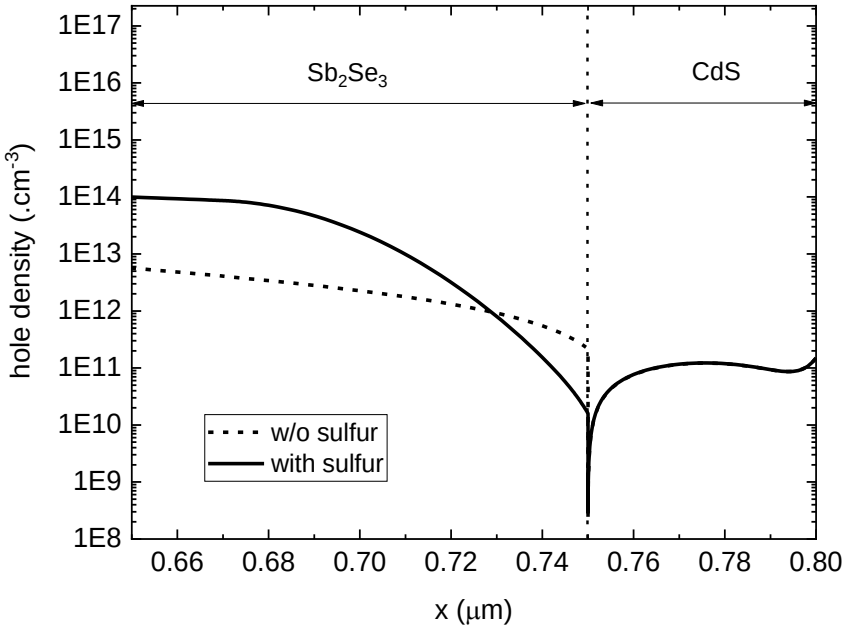


*Figure S 1 Calculated spatial hole density at the vicinity of the pn interface ($x = 0.75\mu m$) for a 50nm sulfurization depth.*

Kunal.tiwari@upc.edu
Zacharie.jehl@upc.edu

4. Quantum efficiency with $Al_2O_3$

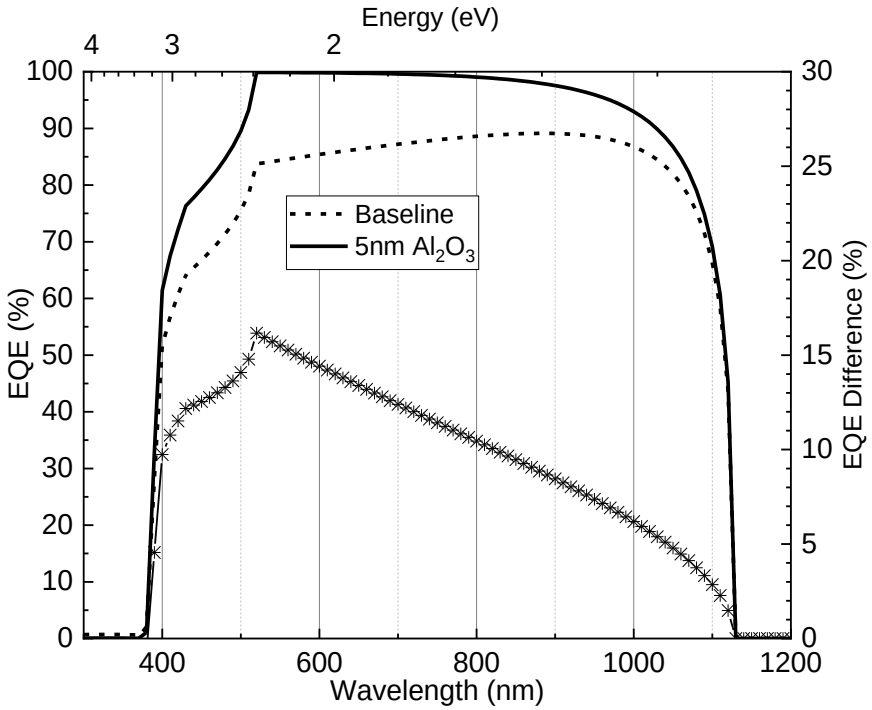


*Figure S 2 Modelled EQE curves comparing the baseline $Sb_2Se_3$ conditions with the passivating 5nm $Al_2O_3$ conditions. The EQE difference is also shown on the right hand y-axis.*


Kunal.tiwari@upc.edu
Zacharie.jehl@upc.edu